Research paper

Time-resolved schlieren observations of shock-induced combustion around a high-speed spherical projectile

Shinichi Maeda*†, Shoichiro Kanno*, Isshu Yoshiki*, and Tetsuro Obara*

*Graduate School of Science and Engineering, Saitama University, 255 Shimo-Okubo, Sakura-ku, Saitama-shi, Saitama 338-8570, JAPAN
Phone : +81-48-858-3445
†Corresponding author : shinichi_maeda@mech.saitama-u.ac.jp

Received : May 17, 2016 Accepted : September 27, 2016

Abstract

Shock-induced combustion around a supersonic spherical projectile was experimentally investigated by high-time-resolution schlieren imaging using a high-speed camera. A projectile of 4.76 mm diameter was launched by a gas gun into a $C_2H_4+3O_2+12Ar$ mixture with the initial pressure varied between 25 and 150 kPa. The Mach number of the projectile ranged from 4.0 to 5.9, which corresponded to 0.7 to 1.1 times the propagation Mach number of the Chapman-Jouguet (C-J) detonation (C-J detonation Mach number). Various combustion regimes, including combustion instabilities with an oscillating combustion front, were observed, and the trend of these regimes was validated using the parameters of a chemical reaction and propagation of the pressure wave driven by a chemical reaction behind the shock wave on the stagnation streamline. Heat release rate parameter, q^* was defined as the maximum temperature gradient in a reaction zone divided by a post-shock temperature assuming a constant-volume explosion, and the time scale, t^* for propagation of the pressure wave was defined as the projectile diameter divided by the difference between a sound speed and a flow velocity at a post-shock state. When the Mach number of the projectile exceeded approximately 0.9 times the C-J detonation Mach number, the induction length was considerably shorter than the scale of the projectile. In this case, the observed combustion regimes tended to exhibit oscillating combustion with a larger scale as the dimensionless heat release rate parameter became larger, which was defined as the product of the q^* and t^*. This trend was in accordance with the one-dimensional consideration of the stagnation streamline in previous numerical studies using hydrogen-fueled mixtures. This was also confirmed by directly observing that the bow shock on the stagnation streamline was temporally oscillating by coupling with the rapid reaction. In contrast, when the Mach number of the projectile was approximately 0.7 to 0.8 times the C-J detonation Mach number, the induction length was comparable with the scale of the projectile. In this case, the mode of oscillating combustion did not exhibit a specific trend when plotted against the dimensionless heat release rate parameter. These experimental results revealed that one-dimensional considerations are insufficient for determining the combustion regime. The observed combustion regime also indicated that the evolution of the reaction front was probably affected by the flow field formed by the aft body of the projectile.

Keywords : supersonic spherical projectile, shock-induced combustion

1. Introduction

The combustion phenomena formed by shock ignition are often called shock-induced combustion and have potential use in the hypersonic propulsion system known as the shock-induced combustion ramjet (Shcramjet)[1]. Fundamental investigations of the combustion phenomena[2)-5)] have been experimentally conducted by launching a supersonic projectile into a combustible mixture at rest. The shock-induced combustion around a blunt-nosed projectile is specifically characterized by

combustion instabilities with an oscillating combustion front, which are observed when the Mach number of the projectile is close to the propagation Mach number of the Chapman-Jouguet (C-J) detonation (called as "C-J detonation Mach number" in this paper). The mechanism of oscillating combustion[2),3)] was suggested to be a one-dimensional wave interaction on the stagnation streamline of the projectile. The pressure wave driven by the chemical reaction interacts with the upstream bow shock, and the periodic amplification and attenuation of the bow shock lead to the periodic variation of the induction time, which forms the oscillations of the reaction boundary. This model well explained the general trends of the frequency of oscillating combustion observed in experiments. The modes of periodically oscillating combustion have been classified[3)] into the "regular regime" of a high-frequency mode with a low amplitude and the "large disturbance regime" of a low-frequency mode with a large amplitude. Such instabilities formed by one-dimensional interactions between the shock and the reaction wave are the fundamental phenomenon used for illustrating the instabilities of one-dimensional detonation[6),7)]. In the 1990s, numerical investigations[8)–10)] reproduced the combustion instabilities of the low- and high-frequency modes, and revealed further details of the mechanisms of the instabilities. Matsuo and Fujii[10)] suggested that the temperature gradient in the reaction zone on the stagnation streamline is an important factor for distinguishing the mode of oscillating combustion. A larger temperature gradient (more rapid reaction) drives a stronger pressure wave to the upstream bow shock, and thus forms combustion instabilities with a larger scale. The experimental, theoretical and numerical works of the shock-induced combustion (including the detonation initiation) by the projectile have been conducted worldwide, and they were reviewed in the literature[11)].

The previous experimental and numerical studies were mainly conducted using hydrogen-fueled combustible mixtures and focused on cases where the Mach number of the projectile was close to the C-J detonation Mach number. Recently, the initiation and stabilization of oblique detonation waves have been experimentally investigated[12)–14)] with the Mach number of the projectile much higher than the C-J detonation Mach number using sufficiently reactive mixtures; however, experimental investigations focusing on shock-induced combustion have hardly been conducted since the 1990s. It is important to investigate shock-induced combustion in a wide range of Mach numbers and in hydrocarbon-fueled mixtures when we seek to apply combustion processes.

The purposes of the present study are as follows. The general trend of the combustion regime against the initial pressure in an ethylene-fueled combustible mixture was investigated and validated using the parameters of the chemical reaction and propagation of the pressure wave behind the shock wave on the stagnation streamline. The temporal evolution of the coupling between the bow shock and the reaction in the large-amplitude mode was directly examined by high-time-resolution schlieren observation. We also investigated the effect of a lower Mach number of the projectile of less than 0.9 times the C-J detonation Mach number, which was investigated in most of the previous studies.

2. Experimental setups and conditions

The experimental apparatus is shown in Figure 1. The projectile was launched from the launch tube (1) of a gas gun, which was driven by a gaseous detonation[15)]. The projectile first entered the blast tube (2) in order to separate the projectile from the muzzle gas flow, and broke diaphragm 1 (polyethylene, 25 μm thickness) to enter the observation chamber (3). The blast tube had a pair of small glass windows through which a diode laser passed through the flight trajectory of the projectile. On the opposite side of the laser, the light intensity was measured using a photodiode to detect the laser-cut signal of the free-flight projectile. The observation chamber was filled with a combustible mixture at the given initial pressure, and had a pair of glass windows for optical access. A schlieren system and a high-speed camera (ULTRA Cam HS-106E, NAC Image Technology Inc.) visualized the flow field around the projectile. The schlieren system was conventional one which consisted of a flash lamp, a pin-hole, two concave mirrors, a schlieren knife edge and an imaging lens. The schlieren knife edge cut vertically a light source image against the flight direction (z direction in Figure 1) of the projectile. Therefore, dark or bright lines in the schlieren image show negative or positive values of $\partial\rho/\partial z$, respectively, where ρ is a density. The center of the visualized region was located about 290 mm downstream of diaphragm 1. The high-speed camera was triggered by the laser-cut signal in the blast tube. Finally, the projectile broke diaphragm 2 (polyethylene, 25 μm thickness) and entered the evacuation chamber (4).

The projectile was a polyethylene sphere with a 4.76 mm diameter in all the experiments. The combustible mixture was stoichiometric ethylene-oxygen diluted with argon with a 75% volumetric fraction. The mixture was preliminarily prepared in a mixture tank using the method of partial pressure, and put about one day in order to mix the gases by molecular diffusion. The mixture was transferred to the observation chamber from the mixture tank in each experiment. The mixture used in the present

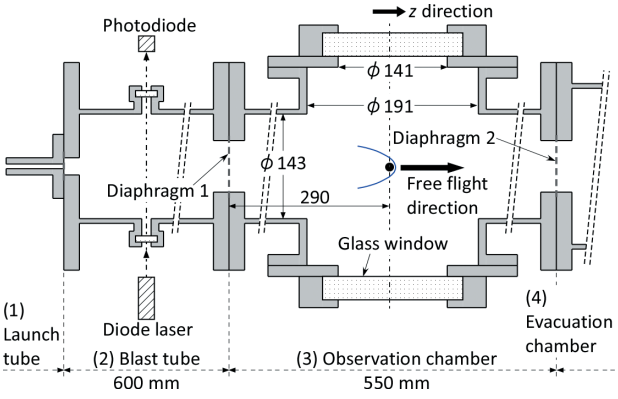

Figure 1 Schematic of experimental apparatus.

study had low effective activation energy compared to that of conventional fuel-air mixtures because of the large amount of argon dilution. In this sense, the tested mixture was not realistic for operation of the Shcramjet engine. The present study aimed to observe the combustion instabilities in the wide range of projectile Mach number for the fundamental investigation. Therefore, the mixture was chosen so as to lower the C-J detonation Mach number and to obtain high post-shock temperatures for given projectile Mach numbers. Figure 2 shows the experimental conditions expressed as the Mach number of the projectile and the initial pressure of the combustible mixture. The C-J detonation Mach numbers for each initial pressure calculated by chemical equilibrium software[16] are also shown in Figure 2. The symbols in the figure denote the observed combustion regimes, which are explained later. The initial pressure of the mixture was varied from 25 to 150 kPa and the initial temperature was room temperature (297 ± 1K). The Mach number of the projectile ranged from 4.0 to 5.9, which corresponded to 0.7 to 1.1 times the C-J detonation Mach number. The initiation of a self-propagating detonation wave was not observed under all conditions. The recording conditions of the high-speed camera were a 2 μs framing speed, 100 ns exposure time and 0.2 mm / pixel spatial resolution. The high-speed camera was able to capture numerous time-resolved schlieren images around the projectile. This allowed us to evaluate whether the observed combustion regime was steady or transient inside the visualized region. The projectile velocity was determined using these

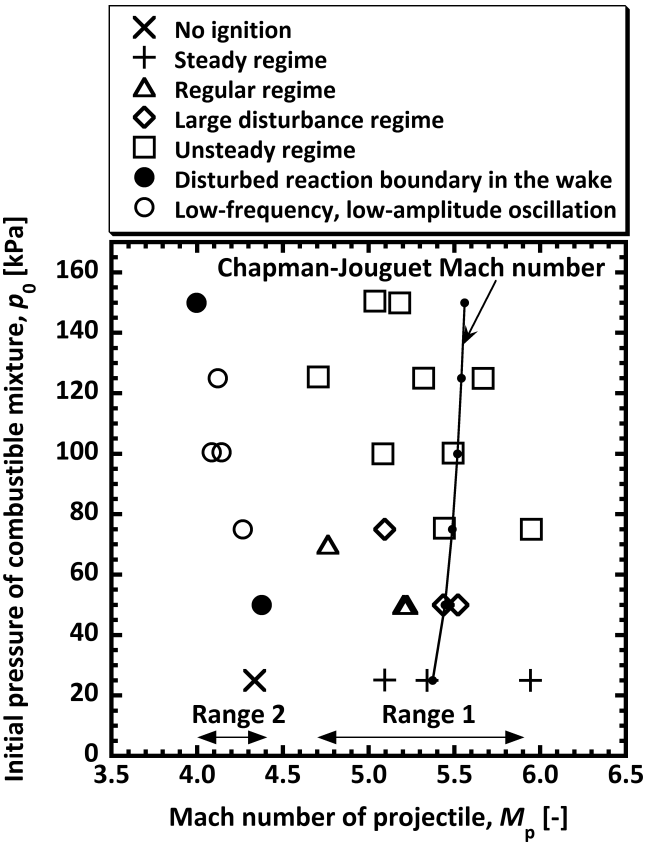

Figure 2 Observed combustion regime for each Mach number of the projectile and initial pressure of the combustible mixture.

continuous images, and the location of the projectile varied almost linearly over time, and thus the velocity deficits in the visualized region were negligible. In the following sections, the observed combustion regimes are first discussed in range 1 (4.7 to 5.9) then in range 2 (4.0 to 4.4) of the Mach number, as shown in Figure 2, then the general trend of the combustion regimes is discussed by considering the thermodynamic and chemical parameters behind the shock wave on the stagnation streamline.

3. Results and discussion

3.1 Observed combustion regimes

Figures 3a-d show the four types of combustion regime observed in range 1 of the Mach number. The initial pressure of the combustible mixture increases from Figure 3a to Figure 3d while keeping the Mach number of 5.1 ± 0.1. The black circle in each image is the spherical projectile. In Figure 3a (steady regime), the steady reaction boundary behind the bow shock is visible in the vicinity of the projectile on the downstream side. The brightness and contrast of the image in Figure 3a were adjusted, because it was difficult to distinguish the reaction boundary in the original image. This steady combustion regime was observed at a low initial pressure (plus symbols in Figure 2). The periodically oscillating reaction boundary shown in Figure 3b was observed at elevated initial pressures (triangles in Figure 2). The schlieren image of the oscillating combustion was characterized by the corrugated reaction boundary. The corrugation of the reaction boundary was segmented by the vertical line of density gradient, which was due to that the corrugation was superposed along the light beam of the schlieren system. One of the segmented reaction boundaries was the evidence for the single cycle of the oscillating combustion. The frequency of oscillation was comparatively high (1 to 2 MHz), which was calculated by dividing the horizontal width of segmented reaction boundary by the projectile velocity, and the vertical width of reaction boundary was comparatively small. This combustion regime is similar to the so-called "regular regime" observed in previous studies[2)-5)]. Another combustion regime with periodic oscillation, as shown in Figure 3c, was also observed when the initial pressure or Mach number was increased from the values for which the regular regime was observed (diamonds in Figure 2). The frequency of oscillation was comparatively low (0.6 to 0.8 MHz) and the vertical width of reaction boundary was comparatively large. This combustion regime is similar to the so called "large disturbance regime" in previous studies[2)-5)]. Each frame of the continuous images showed almost the same flow field in each combustion regime in Figures 3a-c. Therefore, these regimes were steady or periodic combustion regimes within the visualized region. The period of oscillation was comparable to the ignition delay time at the post-shock state on the stagnation streamline for Figure 3b, and was about five times the ignition delay time for Figure 3c (the method for calculating ignition delay times is described in the next section). These results were consistent to the previous

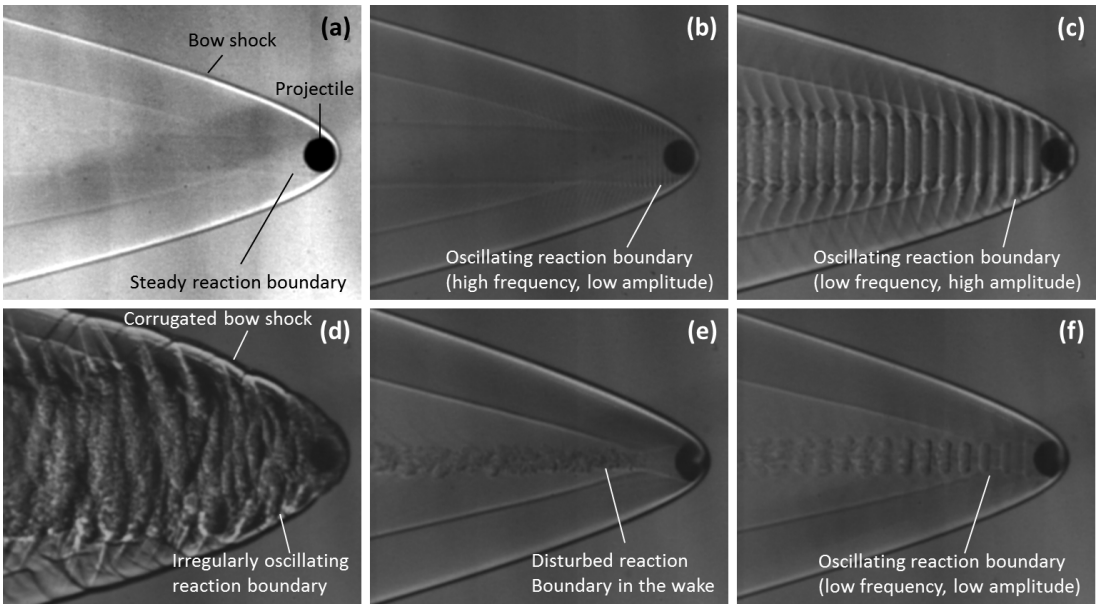

Figure 3 Snapshots of observed combustion regimes. (a) steady regime : $M_p = 5.1$, $p_0 = 25.1$ kPa, (b) regular regime : $M_p = 5.2$, $p_0 = 50.0$ kPa, (c) large disturbance regime : $M_p = 5.1$, $p_0 = 75.0$ kPa, (d) unsteady regime : $M_p = 5.0$, $p_0 = 150.5$ kPa, (e) disturbed reaction boundary in the wake : $M_p = 4.0$, $p_0 = 150.0$ kPa and (f) low-frequency, low-amplitude oscillation : $M_p = 4.3$, $p_0 = 75.0$ kPa (M_p : Mach number of projectile, p_0 : initial pressure of combustible mixture).

experimental and numerical studies[2)−5),8)−10)]. The regime of oscillating combustion was characterized by the strength of the pressure wave driven by the chemical reaction[2),3),9),10)]. Transition between the combustion regimes is considered to be continuous according to the variation of initial conditions such as initial pressures and Mach numbers, because the strength of the pressure wave varies continuously according to the variation of initial conditions. Kasahara et al.[5)] observed the oscillating combustion, in which the high frequency oscillation was superposed on the low frequency oscillation. This regime is probably the intermediate combustion regime of Figure 3b and 3c. In this study, the oscillating combustions in Figure 3b and 3c were categorized as the different regimes according to the previous studies[2)−5),8)−10)], because there was the visible difference between them in terms of the oscillation period and the evolution of the bow shock. The smooth or corrugated bow shock indicated the weak or strong interaction between the bow shock and the chemical reaction for Figure 3b or 3c, respectively. They would show comprehensibly the strength of the pressure wave driven by the chemical reaction. Further increasing the initial pressure resulted in a combustion instability with a larger scale as shown in Figure 3d (squares in Figure 2 : unsteady regime), for which the oscillating reaction boundary did not exhibit a periodic pattern as observed in Figures 3b and 3c. The vertical width of reaction boundary had a larger scale, and a corrugated bow shock was more pronounced than that observed in Figure 3c, which indicated more strong interaction between the bow shock and chemical reaction.

Figure 4 shows time-resolved images of the unsteady regime depicted in Figure 3d. These sequential images clearly show the interaction between the shock wave and the reaction near the stagnation streamline of the projectile. For example, shock wave (a) was pushed up by the chemical reaction in the stagnation streamline at 478 μs and expanded (b) around the projectile along the bow shock at 480 μs. The reaction front was decoupled from the shock front in the subsequent frame and formed the reaction boundary with a large vertical width (c). A similar process was observed from 498 to 502 μs. Such coupling and decoupling of the shock and the reaction front were repeated over time, and they formed the large corrugations of the reaction boundary and the bow shock around the projectile. The numerical simulation of Matsuo and Fujii[9)] indicated that a strong chemical reaction on the stagnation streamline may cause coupling between the shock and the reaction front and initiate a detonation wave. The high propagation velocity of the detonation wave allowed it to penetrate the initial bow shock, and the shock wave in front of the projectile appeared to propagate upstream. Figure 4 gives experimental evidence of this process. The sequential images from 478 to 482 μs and from 498 to 502 μs show the almost symmetric evolution of the shock and the reaction front relative to the stagnation streamline because the interaction between them on the stagnation streamline created axisymmetric evolution. However, the shock fronts around the projectile appeared to undergo asymmetric evolution from 486 to 490 μs. In this oscillating combustion, the strong shock wave coupled with the reaction front was formed, and it interacted with the bow shock, and the bow shock was strongly distorted. This would create multi-dimensional propagations of the strong shock wave ahead of the projectile, which was pointed out by the numerical study of Matsuo and Fujii[9)]. The multi-dimensional wave propagations would strongly affect the evolution of reaction front away from the stagnation streamline. This could cause the asymmetric evolution of

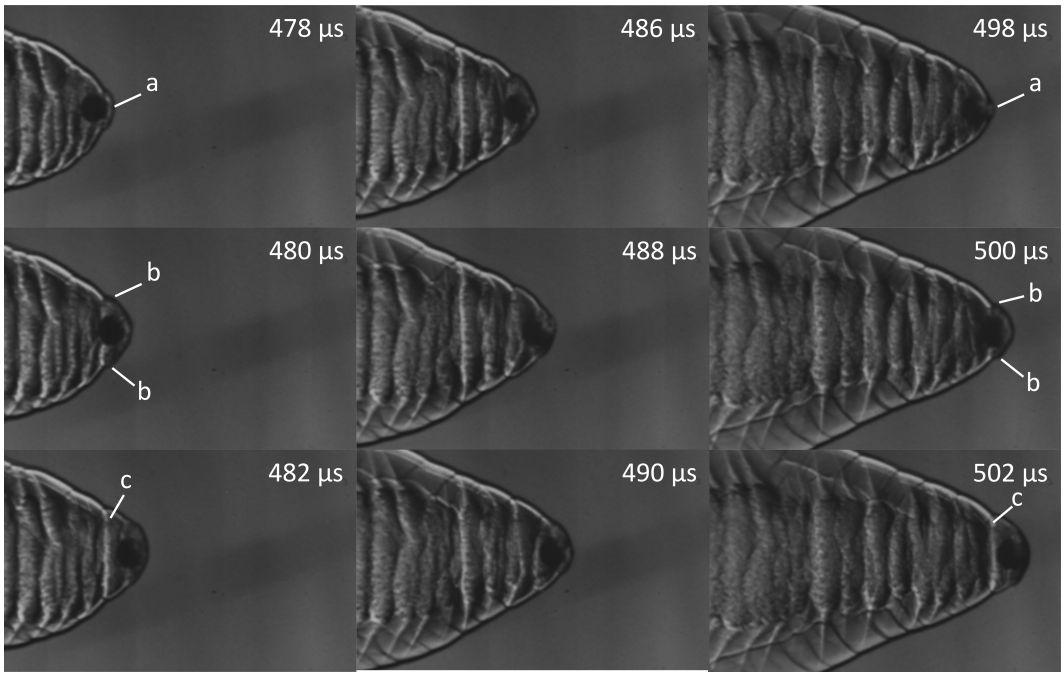

Figure 4 Temporal evolution of unsteady regime depicted in Figure 3d.

the shock and reaction front, which could not be explained only by the one-dimensional wave interaction on the stagnation streamline.

In range 1 of the Mach number, the combustion regime tended to transit from steady combustion to oscillating combustion with a larger scale as the initial pressure increased. This tendency was consistent with that obtained in previous experimental and numerical studies[2)−5),10)] using hydrogen fuel. However, a different tendency was observed at the lower Mach numbers in range 2. At an initial pressure of 25 kPa, no apparent reaction front was observed around the projectile (cross in Figure 2). At initial pressures of 50 and 150 kPa, the reaction boundary existed within a narrow band behind the projectile as shown in Figure 3e (closed circles in Figure 2). Fine disturbances in the narrow reaction boundary were observed downstream of the projectile, which would have been affected by the wake flow behind the projectile. From this observation, a reaction zone should exist along the flow in the immediate vicinity of the projectile surface. At initial pressures of 75 to 125 kPa, a periodically oscillating reaction boundary, as shown in Figure 3f, was observed behind the projectile (open circles in Figure 2). Although the frequency of oscillation (0.3 to 0.5 MHz) was lower than that (0.6 to 0.8 MHz) in the large disturbance regime (Figure 3c), the vertical width of reaction boundary was comparable to the projectile diameter and was smaller than that in the regular regime (Figure 3b). The combustion regimes in Figure 3e and 3f are expected to be related to the increased induction time (enlarged induction length) because of the lower post-shock temperature in the case of a lower Mach number. Interestingly, no variation of the oscillation mode with the initial pressure was observed, which was observed in the higher range of the Mach number.

3.2 Effect of post-shock conditions on stagnation streamline of projectile

The temporal evolution of the gas state along the stagnation streamline of the projectile was simply considered as follows. When viewed from the coordinate system fixed on the projectile, the initial condition for the chemical reaction was the state behind the normal shock wave, which was calculated from the Mach number of the projectile, the initial pressure and the temperature of the combustible mixture. The chemical reaction was assumed to be a constant-volume explosion, as used in the method for predicting the mode of oscillating combustion proposed by Matsuo and Fujii[10)]. The pressure wave generation by the chemical reaction is assumed to be driven by the pressure rise in a constant-volume explosion. The rate of the heat release is used to represent the strength of the pressure wave, which is an important factor affecting the mode of oscillating combustion. In this study, the chemical reaction was calculated using a constant-volume explosion program[17)] and the reaction model of Wang and Frenklach[18)], which was validated by Schultz and Shepherd[17)] by comparison with the induction time data obtained from shock-tube experiments. This combination reproduced the induction times to within about 0.7 to 1.4 times the experimental values for temperatures above 1200 K. Figure 5 shows the typical calculation result for the time histories of the temperature and its gradient during the constant-volume explosion. The origin of the time corresponds to the post-shock state. In this study, the induction time, t_{ind} was defined as that when the temperature gradient reached its maximum value, and the heat release rate parameter, q^* was defined as the maximum temperature gradient divided by the post-shock temperature. The q^* represents that the heat release rate (the rate of the enthalpy increase) per unit mass is normalized by the enthalpy per unit mass at the initial (post-shock) state, assuming the constant specific heat.

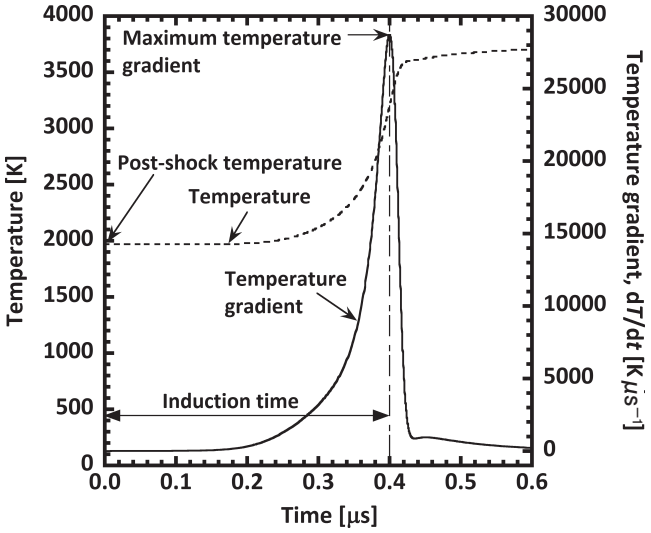

Figure 5 Typical calculation result for the time histories of the temperature and its gradient during the constant-volume explosion. The post-shock pressure and temperature were 2.42 MPa and 1970 K, respectively, which corresponded to the state behind the normal shock wave for a Mach number of 5.09, an initial pressure of 75.0 kPa and an initial temperature of 297 K.

This expression has the same physical meaning as the "chemical characteristic time scale" defined by Matsuo and Fujii[10], which is reciprocal value of the q^*. Another parameter, t^* was used to characterize the time scale for propagation of the pressure wave generated by the chemical reaction. The t^* was defined as the projectile diameter divided by $(a_1 - u_1)$, where a_1 and u_1 were the sound speed and flow velocity at the post-shock state, respectively. The projectile diameter was used simply to characterize the propagation distance of the pressure wave by a shock stand-off distance, because the combustible mixture was not changed and the projectile Mach numbers were the nearly hypersonic region in this study. The $(a_1 - u_1)$ was used to characterize the propagation velocity of the pressure wave, which propagated against the flow velocity behind the shock wave along the stagnation streamline. This expression was the modification of the "characteristic time scale for the fluid part" defined by Matsuo and Fujii[10], in which the projectile diameter was divided by a_1. In this paper, the dimensionless parameter was defined as the product of the q^* and t^*, which would govern the strength of the pressure wave (pressure ratio across the pressure wave) generated by the chemical reaction. This dimensionless parameter characterized the heat release rate and the time scale for the wave propagation, in contrast that the dimensionless parameter in Alpert and Toong[3] characterized the total heat release energy.

Prior to the discussion using the parameters of a chemical reaction, the range of initial conditions of a chemical reaction (thermodynamic states immediately behind the shock wave) is shown. The observed combustion regime is shown in terms of the post-shock temperature and pressure in Figure 6. Because the initial temperature of the combustible mixture was constant at room temperature, the post-shock temperature had a one-

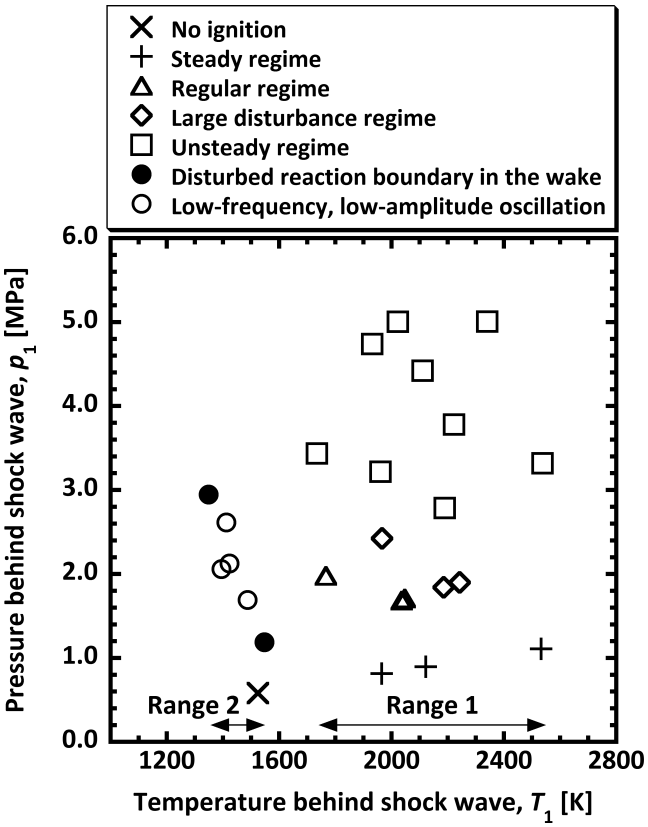

Figure 6 Observed combustion regime for each post-shock temperature and pressure on the stagnation streamline of the projectile.

to-one correspondence with the Mach number of the projectile. The two ranges of the Mach number in Figure 2 are also shown. As shown in Figure 6, in range 1, the combustion regime tended to transit from steady combustion to oscillating combustion with a larger scale with increasing post-shock pressure. However in range 2, the mode of oscillating combustion did not exhibit a specific trend against the post-shock pressure. The trend in range 1 and the difference between range 1 and 2 in terms of the post-shock state are discussed below using the parameters of a chemical reaction.

Next, the observed combustion regime is shown in terms of the post-shock pressure and the dimensionless heat release rate parameter, q^*t^* in Figure 7. Although a large variation of the post-shock temperature is included in this figure, the plots almost lie on a single line and the dimensionless heat release rate parameter is proportional to the post-shock pressure. Therefore, in range 1, the combustion regime tended to transit from steady combustion to oscillating combustion with a larger scale with increasing dimensionless heat release rate parameter. The value of t^* did not vary significantly compared to the variation of the value of q^*, because the projectile diameter were constant and the projectile Mach numbers were the nearly hypersonic region in this study. Therefore, the almost proportional variation of q^*t^* to the post-shock pressure, p_1 was due to that of q^*. From Figure 6, the mode of oscillating combustion seems to simply depend on the value of p_1 in range 1. However, the values of p_1 dividing the mode of oscillating combustion will not be valid, if combustible mixtures and projectile diameters

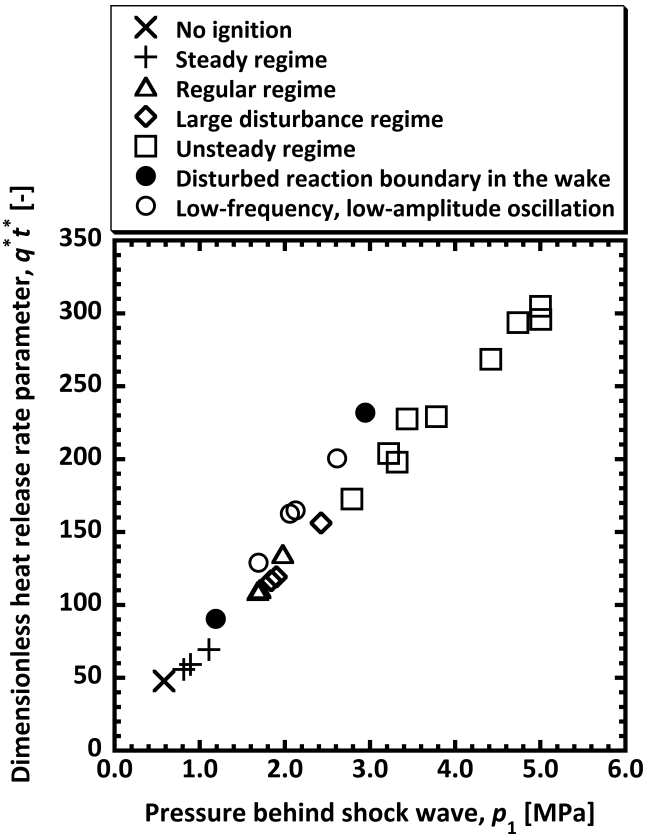

Figure 7 Observed combustion regime for each post-shock pressure and dimensionless heat release rate parameter on the stagnation streamline of the projectile.

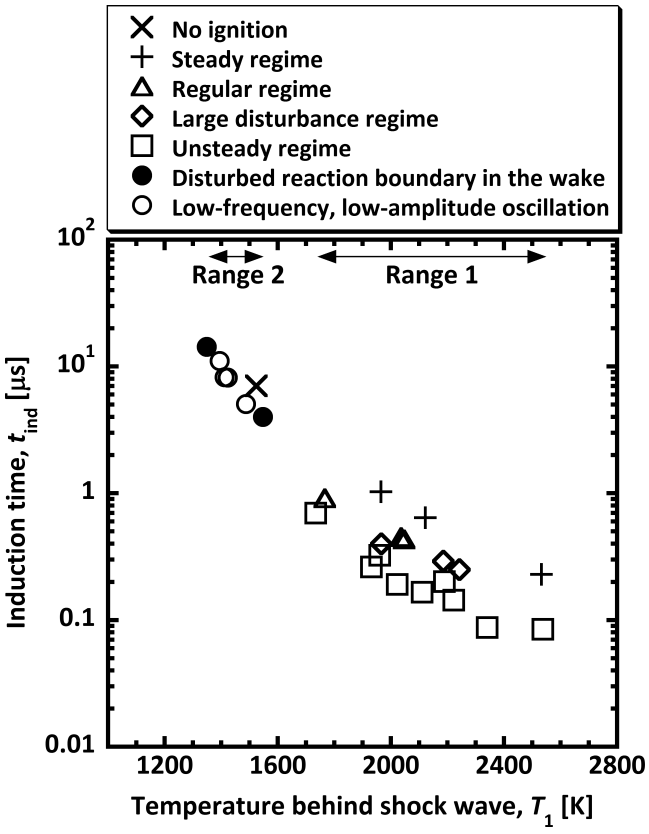

Figure 8 Observed combustion regime for each post-shock temperature and induction time on the stagnation streamline of the projectile.

are changed. Although the results of the present study obtained under the constant mixture composition and the constant projectile diameter cannot give the experimental evidence for whether the dimensionless parameter, q^*t^* is the governing parameter for determining the mode of oscillating combustion, this dimensionless parameter is more reasonable than p_1, because it characterizes the heat release rate and the time scale for the wave propagation supported by the numerical results of Matsuo and Fujii[10].

Finally, the observed combustion regime is shown in terms of the post-shock temperature and the induction time in Figure 8. The two ranges of the Mach number are also shown. From this figure, the induction time strongly depended on the temperature as an exponential function and also had a measurable dependence on the pressure; therefore, the results did not lie on a single line as in Figure 7. The maximum and minimum induction times had about a hundredfold difference, whereas the dimensionless heat release rate parameters had about a tenfold difference. The induction times were on the order of 10 μs in range 2 of the Mach number and on the order of 0.1 to 1 μs in range 1. If the induction lengths on the stagnation streamline are roughly estimated by simply multiplying the flow velocity behind the shock wave and the induction time, although in reality the flow behind the shock wave is considered to decelerate toward the head of the projectile, the estimated induction lengths are within 1.2 to 4.2 mm in range 2 and within 0.03 to 0.34 mm in range 1. Because the Mach number of the projectile was above 4 in the nearly hypersonic region, the flow velocity behind the shock wave did not change significantly with the Mach number and fell within 300 to 360 ms^{-1}. Measurement of the shock stand-off distance from the obtained schlieren images, as shown in Figure 3, was difficult owing to the limited spatial resolution; however, the shock stand-off distances were clearly smaller than the estimated induction lengths in range 2, which were comparable to the projectile radius or diameter. This indicates that the pressure wave driven by the chemical reaction cannot effectively interact with the upstream bow shock on the stagnation streamline. The one-dimensional consideration using the dimensionless heat release rate parameter on the stagnation streamline should be valid when the induction length is sufficiently shorter than the projectile diameter as in range 1, where the Mach number is close to the C-J detonation Mach number. The results of the present study revealed that the one-dimensional consideration is insufficient to classify the combustion regime when the induction length is on the order of the projectile diameter as in range 2. Regarding the combustion regime in Figure 3e, in which the reaction boundary was entrained in the wake flow behind the projectile, the evolution of the reaction front was probably affected by the flow field formed by the aft body of the projectile because of the elongated induction length due to the low post-shock temperature.

4. Conclusions

Various combustion regimes around a supersonic spherical projectile in an ethylene-fueled combustible

mixture were observed by high-time-resolution schlieren imaging, and the following conclusions were obtained.

When the Mach number of the projectile exceeded approximately 0.9 times the C-J detonation Mach number, the observed combustion regimes tended to show oscillating combustion with a larger scale as the dimensionless heat release rate parameter became larger. These experimental results indicated that the one-dimensional consideration on the stagnation streamline in previous numerical studies using hydrogen-fueled mixtures is valid when the induction length is sufficiently shorter than the scale of the projectile. Under these conditions, it was directly observed that the bow shock on the stagnation streamline temporally oscillated by coupling with the rapid reaction, and a large segmented reaction boundary was formed.

When the Mach number of the projectile was approximately 0.7 to 0.8 times the C-J detonation Mach number, the mode of oscillating combustion did not exhibit a specific trend against the dimensionless heat release rate parameter. This revealed that the one-dimensional consideration is insufficient for determining the combustion regime when the induction length is comparable to the scale of the projectile. In this case, the observed phenomena indicated that the evolution of the reaction front was probably affected by the flow field formed by the aft body of the projectile because of the elongated induction length due to the low post-shock temperature.

Acknowledgements

This work was supported by JSPS KAKENHI Grant Number 26870096.

Reference

1) J.P. Sislian, R.P. Martens, T.E. Schwartzentruber, and B. Parent, J. Propul. Power, 22, 1039−1048 (2006).
2) J.B. McVey and T.Y. Toong, Combust. Sci. Tech., 3, 63−76 (1971).
3) R.L. Alpert and T.Y. Toong, Astronaut. Acta., 17, 539−560 (1972).
4) H.F. Lehr, Astronaut. Acta, 17, 589−597 (1972).
5) J. Kasahara, T. Horii, T. Endo, and T. Fujiwara, Proc. Combust. Inst., 26, 2903−2908 (1996).
6) W. Fickett and W.C. Davis, "Detonation - Theory and Experiment", 312, Dover Publications, New York (2000).
7) C.K. Law, "Combustion Physics", 666, Cambridge University Press, New York (2006).
8) G.J. Wilson and M.A. Sussman, AIAA J., 31, 294−301 (1993).
9) A. Matsuo and K. Fujii, AIAA J., 33, 1828−1835 (1995).
10) A. Matsuo and K. Fujii, AIAA J., 36, 1834−1841 (1998).
11) M.J. Kaneshige, "Gaseous Detonation Initiation and Stabilization by Hypervelocity Projectiles", 15−37, Ph.D. Thesis, California Institute of Technology, (1999).
12) J. Kasahara, T. Arai, S. Chiba, K. Takazawa, Y. Tanahashi, and A. Matsuo, Proc. Combust. Inst., 29, 2817−2824 (2002).
13) J. Verreault and A.J. Higgins, Proc. Combust. Inst., 33, 2311−2318 (2011).
14) S. Maeda, S. Sumiya, J. Kasahara, and A. Matsuo, Shock Waves, 25, 141−150 (2015).
15) S. Maeda, S. Kanno, R. Koto, and T. Obara, Trans. JSME, 81 (DOI : 10.1299/transjsme.14−00332) (2015) (in Japanese).
16) S. Gordon and B.J. McBride, "Computer Program for Calculation of Complex Chemical Equilibrium Compositions and Applications", NASA Reference Publication 1311 (1994).
17) E. Schultz and J. Shepherd, "Validation of Detailed Mechanisms for Detonation Simulation", Explosion Dynamics Laboratory Report FM99−5, GALCIT (2000).
18) H. Wang and M. Frenklach, Combust. Flame, 110, 173−221 (1997).